Applied Catalysis B: Environmental 84 (2008) 766–772

Contents lists available at ScienceDirect

Applied Catalysis B: Environmental

journal homepage: www.elsevier.com/locate/apcatb

Reactive adsorption of thiophene on Ni/ZnO: Role of hydrogen pretreatment and nature of the rate determining step

Andrey Ryzhikov, Igor Bezverkhyy *, Jean-Pierre Bellat

Institut Carnot de Bourgogne, UMR 5209, CNRS-Université de Bourgogne, 9 av. A. Savary, BP 47870, 21078 Dijon Cedex France

ARTICLE INFO

Article history:
Received 7 May 2008
Received in revised form 10 June 2008
Accepted 11 June 2008
Available online 18 June 2008

Keywords:
Thiophene adsorption
Reactive adsorption
ZnO-supported Ni

ABSTRACT

Reactive adsorption of thiophene on reduced and unreduced NiO/ZnO adsorbents was studied by thermal gravimetric analysis and by sulfidation in a fixed bed reactor at 330–375 °C and 10–40 mbar of thiophene in hydrogen. The adsorbents (12 wt% Ni) were prepared by co-precipitation of corresponding nitrates with sodium carbonate followed by calcination at 400 °C. We have found that such solids can react with thiophene without any prior reduction. Metallic Ni, indispensable for thiophene decomposition, is formed in this case *in situ* upon the contact with thiophene/H_2 reaction mixture. The reduction of NiO/ZnO in H_2 (360 °C, 6 h) results in the formation of Ni–Zn alloyed particles (as attested by XRD data) and leads to a decrease of the sulfidation rate in comparison with the unreduced sample. Concerning the mechanism of the reaction, we found that H_2S is absent in the gas phase during sulfidation in a fixed bed reactor for both reduced and unreduced solids, showing that all produced H_2S is rapidly absorbed by ZnO. This observation points out that catalytic thiophene decomposition on Ni is the rate determining process under used conditions. Existence of two stages in the reactive adsorption, characterized by different rates and activation energies, is explained by the change of the rate determining step of thiophene decomposition from desulfurization reaction itself in the first stage to thiophene transport in the second one. Based on these findings we attributed the lower reaction rate of the reduced sample to a lower activity and/or accessibility of metallic Ni in such adsorbents.

1. Introduction

Deep desulfurization of hydrocarbon-containing gases, used either as raw materials in petrochemical industry or as fuels, is one of the most urgent and challenging tasks in modern technology. This importance is due to strong poisoning effect of sulfur for metallic catalysts whatever their application field is: oxidation of car exhaust gases in a catalytic converter, hydrogen production in a steam reformer or electricity production in a fuel cell. Absorption, adsorption or catalytic approaches are used for desulfurization depending on the nature of sulfur species and composition of the stream. Thus, H_2S can be eliminated by washing with basic solvents or by reacting with ZnO [1]. The latter approach is widely applied for the finishing treatment of the gases used for hydrogen production by hydrocarbon steam reforming as it allows to achieve residual sulfur level as low as 0.02 ppm [2]. In contrast, aromatic sulfur-containing molecules (thiophenes or dibenzothiophenes), present in oil, cannot be eliminated in this way and catalytic hydrodesulfurization (HDS) process is used in refineries to achieve a low level of sulfur in fuels [3].

Due to more stringent recent environmental norms, many new approaches based either on adsorption or on oxidation of sulfur-containing species have recently been proposed [4]. One of them, reactive adsorption of sulfur-containing molecules, combines in one solid a catalyst of HDS and ZnO adsorbent to absorb H_2S formed in the reaction [5]. This approach brings together advantages of catalytic and adsorption technologies. It allows to remove rather stable compounds like thiophene and in the same time to achieve very low S concentration limited only by ZnO sulfidation equilibrium. Despite these valuable properties of the reactive adsorption, its mechanism has not yet been characterized.

In our previous article [6] we have used thermal gravimetric analysis to study kinetics of the interaction between a model adsorbent Ni/ZnO and thiophene. It was shown that sulfidation of reduced Ni/ZnO follows a reaction pattern consisting of two major stages. The first one gives an S-shaped thermal gravimetric analysis (TGA) profile characteristic of nucleation-controlled reactions and the second, slower one, has a nearly constant reaction rate. Both

* Corresponding author. Tel.: +33 380 39 60 38; fax: +33 380 39 61 32.
E-mail address: Igor.Bezverkhyy@u-bourgogne.fr (I. Bezverkhyy).

0926-3373/$ – see front matter © 2008 Elsevier B.V. All rights reserved.
doi:10.1016/j.apcatb.2008.06.009

stages have a first-order kinetics relatively to thiophene concentration, but the activation energy of the first stage is greater than the second one.

The present work is a continuation of the first study and it had two aims: (i) to elucidate the nature of the rate determining steps for both stages and (ii) to characterize how hydrogen pretreatment of NiO/ZnO influences the kinetics of the reactive adsorption. To achieve the first aim we studied the evolution of the reaction products (H_2S and butenes) during sulfidation in a fixed bed reactor in order to correlate the trends with different reaction steps observed in the TGA conversion profiles. Concerning the role of hydrogen pretreatment, we characterized the kinetics of a *direct* interaction between thiophene and NiO/ZnO without any prior pretreatment in H_2.

2. Experimental

2.1. Sample preparation and characterization

$Zn(NO_3)_2{\cdot}6H_2O$ and $Ni(NO_3)_2{\cdot}6H_2O$ of reactive grade (Aldrich) were used for preparation of Ni/ZnO samples by co-precipitation with sodium carbonate. 6.576 g (0.0221 mol) $Zn(NO_3)_2{\cdot}6H_2O$ and 1.556 g (0.0054 mol) $Ni(NO_3)_2{\cdot}6H_2O$ were dissolved in 137.5 mL of water to obtain 0.2 M solution. Taken quantities correspond to 20 wt% of NiO in NiO/ZnO sample. Co-precipitation was done by drop wise addition of equimolar quantity of 0.5 M solution of Na_2CO_3 under vigorous stirring. Obtained suspension was stirred during 12 h, and then the solid was filtered, thoroughly washed with water and dried in oven overnight at 100 °C. After drying the sample was annealed in air at 400 °C for 4 h (heating rate: 2 °C/min). For characterization purposes a part of the sample was reduced in hydrogen at 360 °C for varying time. After such treatments the solids were passivated by purging reactor with nitrogen and then adding progressively air in the N_2 flow.

X-ray diffraction patterns of the samples were recorded using an INEL CPS120 curved detector with Cu Kα monochromatic radiation. Transmission electron microscopy micrographs were obtained on a JEOL JEM 2100 instrument. BET surface areas were measured on a BEL mini apparatus by N_2 adsorption at 77 K. Chemical analysis of the samples was done by ICP after dissolving the sample in 2% HNO_3 solution.

2.2. Thermal gravimetric analysis (TGA)

To characterize reaction kinetics by TGA, a homemade setup was used, in which the sample weight was recorded with a SETARAM B85 balance head (Fig. 1). The gas supply was made in a way to permit reduction of the sample before the reaction and the gas lines for reduction and reaction (correspondingly "H" and "S" on the scheme) were separated to avoid any contamination of pure H_2 by sulfur species. The sample was suspended in a silica tube in which a bottom-up gas flow passed and the measurement head was continuously purged with nitrogen. The thiophene/H_2 reaction mixture was obtained by passing hydrogen through a saturator containing liquid thiophene at desired temperature. Before the reaction the NiO/ZnO solids issued from calcination were pretreated in two different manners. They were either heated in N_2 flow (150 mL/min) for 1 h at 360 °C or reduced in H_2 flow at 360 °C for 6 h. Preliminary experiments showed that use of gas flow greater than 130 ml/min and sample mass lower than 30 mg allows to exclude any influence of mass transfer in gas phase and between the powder particles. Therefore, the hydrogen flow of 150 ml/min and samples of 20 mg were used systematically throughout this study.

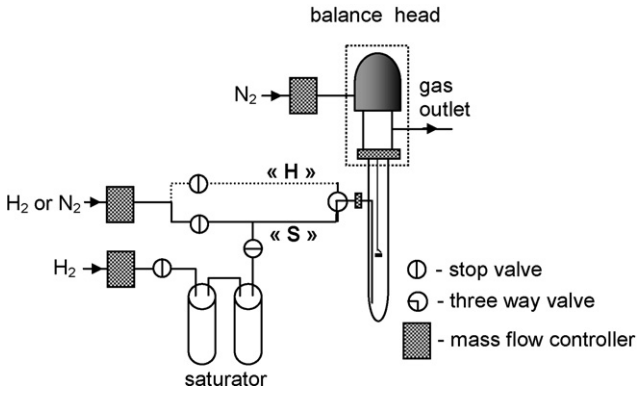

Fig. 1. Scheme of the TGA setup used for recording conversion profiles.

2.3. Sulfidation in a fixed bed reactor

The setup used for fixed bed sulfidation resembles closely a typical installation for gas phase micro-reactor catalytic tests. As in the case of TGA analysis, the gas line for sample reduction was separated from that used for supplying thiophene-saturated H_2 to the reactor. The sample (0.1 g) was placed in a U-tube reactor and pretreated in the same manner as for TGA measurements. Then the thiophene/H_2 mixture was admitted into reactor at 10 ml/min. The mixture from the reactor outlet was injected periodically through a six-way automatic gas valve in the online gas chromatograph (HP 6890) equipped with a mass selective detector. For quantitative analysis the detector was calibrated with standard mixtures containing H_2S or a mixture of butenes in N_2. The ChemStation software package was used for treating obtained chromatographic data.

3. Results

3.1. Sample characterization before and after sulfidation

Some properties of the sample used in the present work are given in Table 1. We used a sample with a higher amount of Ni than in our previous study [6]. Such content is closer to that employed in the adsorbent for which a high efficiency was demonstrated in industrial conditions [5]. Also, a use of the adsorbent with a higher Ni content permitted a more facile characterization of the state of Ni and its role in thiophene reactive adsorption.

As attested by value of BET specific area, the co-precipitation by Na_2CO_3 allows to obtain a highly dispersed solid. The size of crystallites obtained from the measured value supposing spherical particles (i.e. $d = 6/\rho S$) is in poor agreement with that estimated from X-ray diffraction peaks broadening, which can be explained by agglomeration of crystallites or by a polycrystalline nature of the particles. As can be seen from Table 1, reduction treatment results in a decrease of the surface area of the solid. A slight increase of ZnO particles size can only partially explain the observed change. Hence, a pronounced agglomeration during

Table 1
Properties and composition of the samples used in the work

Sample	S_{BET} (m^2/g)	Ni (wt%)	d(Ni)[a] (nm)	d(ZnO)[a] (nm)
NiO/ZnO	60	12.3	5.3[b]	12
Ni/ZnO (reduced at 360 °C in H_2 for 6 h)	34	12.7	6.6[c]	15

[a] Determined from X-ray peak broadening.
[b] Calculated from the size of NiO using molar volumes of Ni and NiO.
[c] Size of Ni–Zn alloy particles.

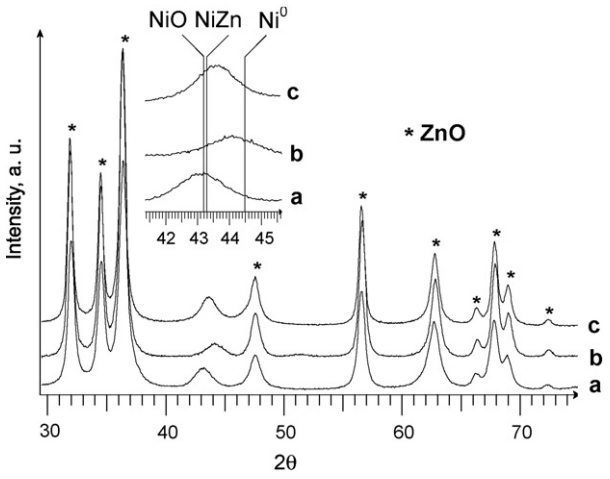

Fig. 2. XRD patterns for NiO/ZnO samples after calcination (a) and after reduction in H_2 at 360 °C for 30 min (b) and for 6 h (c).

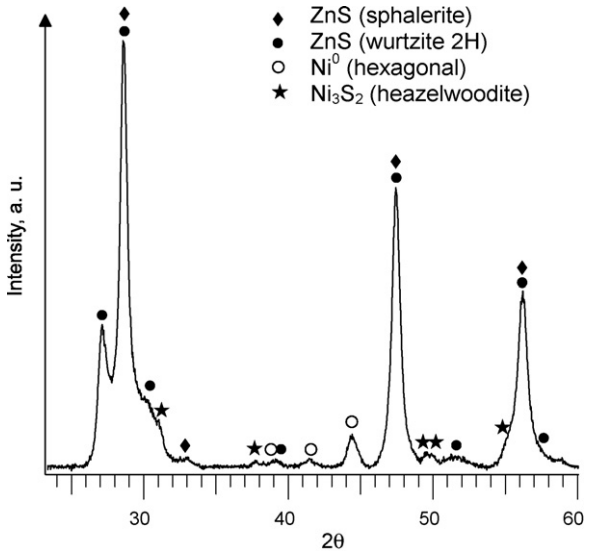

Fig. 3. XRD pattern of the unreduced sample after reaction with thiophene at 360 °C and 20 mbar of thiophene in H_2.

reduction should therefore be supposed, which diminishes the available surface.

XRD pattern of the sample after calcination (Fig. 2a) contains the peaks characteristic of the hexagonal ZnO (JCPDF 00-036-1451). The only additional peak (at $2\Theta = 43.2°$) can be attributed to NiO (JCPDF 00-047-1049), its other peaks being masked by more intense ZnO diffraction maxima. The interpretation of the data for the reduced sample is less straightforward. Indeed, in the sample annealed in H_2 at 360 °C for 6 h we observe a similar additional peak which is slightly displaced to $2\Theta = 43.7°$ (Fig. 2c). Due to this proximity we interpreted it in our previous work as characteristic of NiO formed after reoxidation of the reduced sample in air [6]. Additional data on the reactivity of such samples (see below) and the literature data [7] indicated that the maximum at $2\Theta = 43.7°$ can belong to the pattern of a Ni–Zn alloy, because for NiZn intermetallic compound the most intense peak is situated at $2\Theta = 43.2°$ (JCPDF 00-006-0672). To verify this hypothesis we did a reduction treatment for a shorter time in order to reduce Ni but avoid the alloy formation. The XRD pattern of the sample treated in H_2 for 30 min and passivated (Fig. 2b) confirms our attribution: the peak in this case is situated at $2\Theta = 44.1$ °C which is close to metallic Ni (JCPDF 00-004-0850). It means that Ni^0 particles, formed after short reduction treatment and passivation, are sufficiently stable in air to be detected by XRD and consequently the species obtained after a longer treatment should be metallic Ni–Zn alloy and not NiO.

Quantitative information on the degree of ZnO reduction was obtained from the data on oxidation of these reduced samples in air at 200 °C. Thus, for the sample treated in H_2 at 360 °C for 30 min the weight gain after oxidation is 3.4% (relatively to initial sample weight), which corresponds to a complete oxidation of metallic Ni. In contrast, after 6 h of treatment in H_2 the weight gain is 5.5% corresponding to additional reduction of 13% of ZnO. The obtained alloy is therefore enriched in Ni (Ni/Zn = 1.5 instead of 1), which explains the shift of the peak towards pure Ni (Fig. 2c). In conclusion, the XRD data and oxidation experiments give evidence that a prolonged treatment of Ni/ZnO samples in H_2 at 360 °C leads to a partial reduction of zinc and its alloying with Ni.

After reaction with thiophene a complex XRD pattern (recorded *ex situ*) is observed (Fig. 3). It contains the peaks characteristic of sphalerite (JCPDS 00-005-0566), wurtzite-2H (JCPDS 00-036-1450), metallic Ni (JCPDS 00-045-1027) and Ni_3S_2 (heazlewoodite, JCPDS 00-044-1418). We note that ZnO is completely sulfided, while for nickel the reaction is only partial. Interestingly, after reaction Ni^0 adopts the hexagonal structure rather than the cubic one, observed in the initial sample.

Transmission electron microscopy (Fig. 4) shows that initial sample consists of strongly agglomerated shapeless particles of *ca*. 10–30 nm. The contrast between Ni and Zn is insufficient to distinguish the metals and observed dark spots are not Ni particles as attested by EDX analysis. Sulfidation significantly modifies textural properties of the solid (Fig. 4b): particle size is visibly increased and the smaller particles, observed in the initial sample, disappear. This observation is in line with a decrease of BET surface area after sulfidation from 60 to 26.3 m^2/g for the unreduced sample and from 34 to 17.0 m^2/g for the reduced one. The shape of the particles is also changed after reaction. An irregular corrugated structure of the facets and a strong variation of contrast throughout a particle point out to a polycrystalline nature and a complex morphology of the particles in sulfided solids.

3.2. TGA study of the reaction between Ni/ZnO and thiophene

Before discussing experimental data we would like to make some comments about calculation of the transformation degree for reduced and unreduced samples. Raw gravimetric data for the two samples (including pretreatment) is given in Fig. 5. We note that for the unreduced sample after admitting thiophene/H_2 mixture to the reactor (the point indicated by an arrow) a weight decrease is observed, which represents the difference of two opposing trends. The first one is the weight loss due to reduction of NiO in H_2 and the second one is the increase of the sample weight because of a weaker buoyancy in H_2 than in N_2. The latter effect equals to *ca*. 1% of the weight as determined from the blank experiments. Using this value we estimate that about half of Ni is reduced to Ni^0 upon the contact with the reaction mixture. Supposing that a complete sulfidation would give a mixture of Ni_3S_2 and ZnS, we obtain that the maximum weight increase for such sample should be 19.4%.

It follows from the comparison of the curves that the weight gain for the reduced sample is higher than for the unreduced one (Fig. 5a). The increase can be attributed to sulfidation of Zn^0, formed in the reduced sample. Indeed, during sulfidation of ZnO the measured weight change is the difference between the mass of

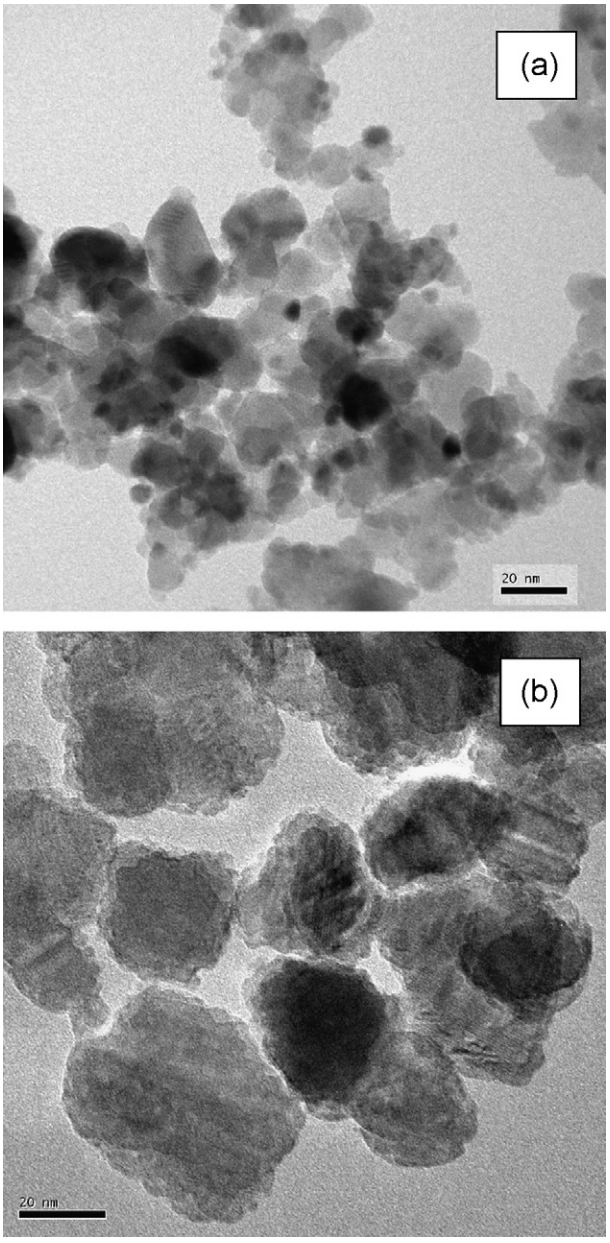

Fig. 4. TEM micrographs of the unreduced sample before (a) and after reaction at 360 °C and 20 mbar of thiophene (b).

absorbed sulfur and that of eliminated oxygen according to the reaction:

$$ZnO + H_2S \rightarrow ZnS + H_2O$$

When metallic zinc is sulfided, the corresponding weight change equals the amount of sulfur combined with Zn^0 to give ZnS. The weight gain per mole of Zn in this case is higher than for ZnO sulfidation, since no oxygen is eliminated. Using the amount of Zn^0 found in oxidation experiments (13%) one can calculate that the maximum weight gain for such sample is equal to 23.2%.

The conversion profiles (transformation degree *vs.* time) calculated with the theoretical maximum weight gains are given in Fig. 5b. These maximum values are used throughout the article to calculate the conversion profiles under other reaction conditions. We note that the transformation degree is lower than unity because of only partial sulfidation of Ni in agreement with XRD data.

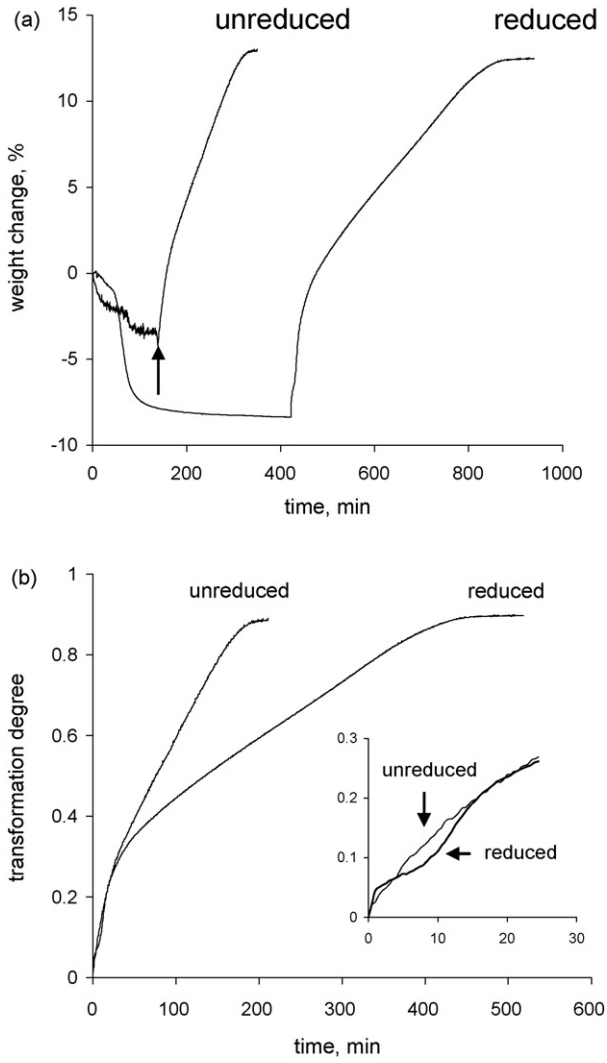

Fig. 5. Conversion profiles of reduced and unreduced samples at 360 °C and 20 mbar of thiophene: raw gravimetric data (a) and corresponding conversion profiles (b) (inset: the first part of the conversion profiles).

The reaction of reduced and unreduced samples with thiophene was studied at different temperatures and thiophene partial pressures (Figs. 6 and 7). In both cases under all conditions two main domains can be distinguished in the conversion profiles: a rapid weight increase to ~0.3 followed by a slower progression. For the reduced sample the first part is preceded by an additional sharp increase (to ~0.05) at the beginning, whose level and rate is independent of the reaction conditions. This fact and existence of a similar step in the case of Ni/SiO_2 permitted us to attribute it to chemisorption of thiophene on reduced metallic particles [6].

The shape of the first part of the reaction profile is different for reduced and unreduced samples. After reduction the profile is S-shaped and can be fitted with the Avram–Erofeev equation in the same way as we have done for Ni/ZnO samples with lower Ni content studied previously [6]. However, in this work in order to compare reduced and unreduced samples we used another parameter to characterize the first stage—its maximum rate, which corresponds to the slope of the middle (linear) part of the curve. For the sample reacting directly, the shape of the first part is characteristic of slowing down reaction whose maximum rate can be determined from the initial slope of the curve. The values of maximum rates of the first stage determined in this way are similar

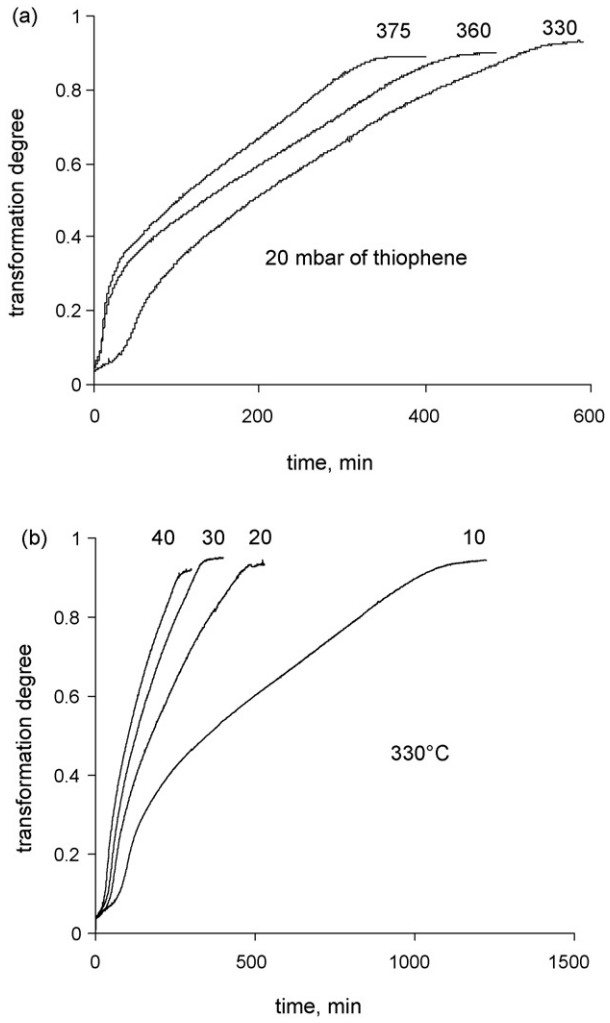

Fig. 6. Conversion profiles of the reduced sample (360 °C, 6 h) at varying temperature (a) and thiophene pressure (b).

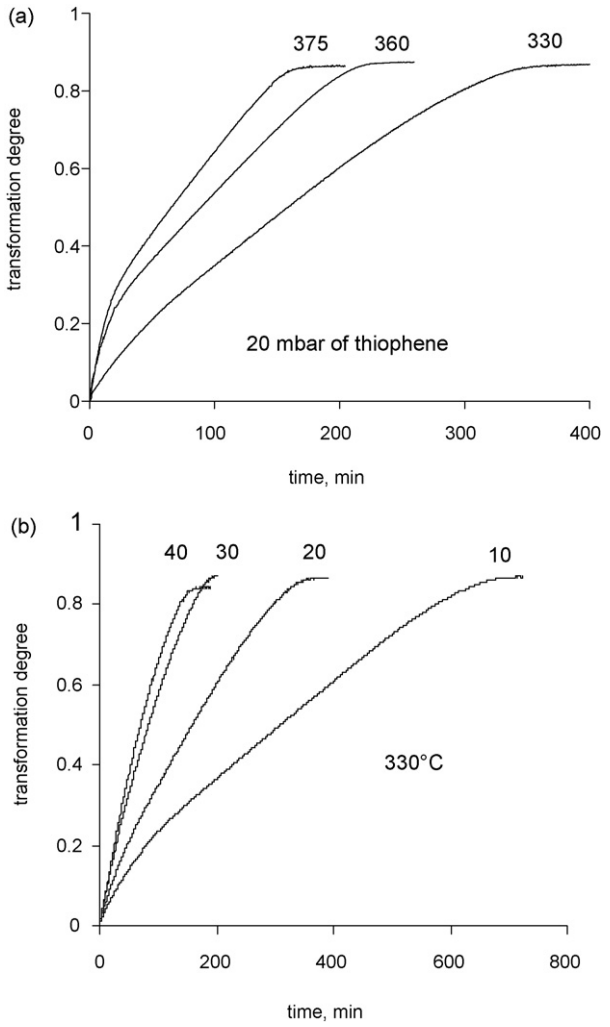

Fig. 7. Conversion profiles of the unreduced sample at varying temperature (a) and thiophene pressure (b).

for reduced and unreduced samples (Table 2). The activation energy calculated from this data is 85 kJ/mol for the unreduced sample and 105 kJ/mol for the reduced one.

The shape of the second part of the reaction profile for both samples is close to linear one (Figs. 6 and 7), thus we used the slope between 0.5 and 0.7 as an estimation of the reaction rate during the second stage (Table 2). We note that the reaction slows down after the first stage, but the decrease of the rate is less pronounced for the unreduced sample so that during the second stage its sulfidation rate is about twice of that for the reduced one. The activation energy of the second stage is equal to 32 kJ/mol for the unreduced sample and to 24 kJ/mol for the reduced one.

3.3. Study of the interaction between thiophene and Ni/ZnO in a fixed bed reactor

Evolution of the concentrations of the gaseous products, formed during reaction, follows similar pattern under all conditions. The representative data for the reduced and unreduced adsorbents at 360 °C and 20 mbar of thiophene is shown in Fig. 8. The major hydrocarbon products are butenes (*trans*-2-butene, *cis*-2-butene and 1-butene), also butane and isobutene are formed in minor quantities. Hydrogen sulfide in the gas phase is observed only after an important lapse of time and after appearance of H_2S all concentrations become constant. This fact allows to conclude that

Table 2
Maximum rates for the first stage (v_I) and the mean reaction rates for the second (v_{II}) stage for the reaction between thiophene and NiO/ZnO samples

Temperature (°C)	Thiophene pressure (mbar)	Reduced		Unreduced	
		v_I ($\times 10^3$ min^{-1})	v_{II} ($\times 10^3$ min^{-1})	v_I ($\times 10^3$ min^{-1})	v_{II} ($\times 10^3$ min^{-1})
375	20	22.8	1.7	18.1	4.1
360	20	16.5	1.4	14.1	3.3
330	20	5.5	1.3	5.7	2.6
300	20	2.5	0.7	3.3	1.5
330	10	3.7	0.6	3.8	1.2
330	30	7.2	2.1	7.5	4.5
330	40	9.1	2.4	7.9	5.6

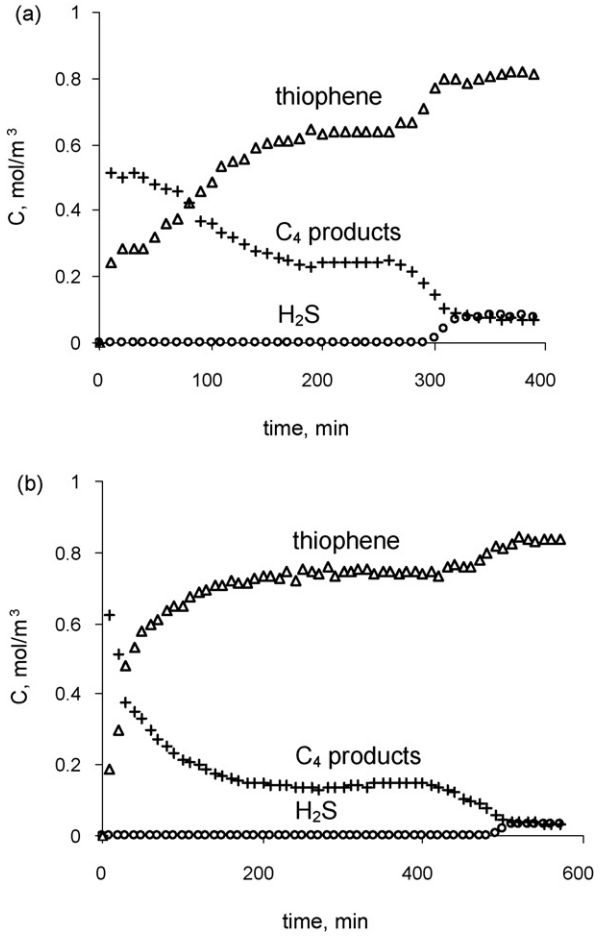

Fig. 8. Evolution of the concentration of the gaseous products during interaction between thiophene and unreduced (a) and reduced (b) NiO/ZnO samples at 360 °C and 20 mbar of thiophene in a fixed bed reactor.

appearance of H_2S in the gas phase coincides with the completion of the sulfidation and thiophene conversion measured in this domain is only due to catalytic desulfurization.

Before the end of the sulfidation, two domains can be clearly distinguished in all curves both for the reduced and unreduced sample. The first one is characterized by initially high but dropping concentration of hydrocarbons and the complementary evolution of thiophene concentration. The second one is a plateau corresponding to constant product concentrations. These two domains can be correlated with two parts of the TGA profiles (Figs. 6 and 7): decrease of product concentrations corresponds to a decelerating reaction (first stage) and their steadiness—to a constant rate weight increase (second stage). The S-shape of the first part of the TGA profiles for the reduced sample is not reflected by the evolution of the products in a fixed bed reactor, because the interval between injections (10 min) is longer than the induction period under these conditions (*ca.* 5 min).

4. Discussion

The data obtained in this work allows to describe some mechanistic features of the reactive adsorption of thiophene on Ni/ZnO. We consider that the most important point is the absence of H_2S in the gas phase until the complete sulfidation of the solid. It means that all free sulfur species, produced from thiophene, react rapidly with the solid, so that H_2S cannot desorb from the surface into the gas phase. In other words, sulfidation of ZnO is more rapid than thiophene desulfurization, which appears thus to be the rate determining process for both stages of the reaction.

Another important observation concerns the role of Ni. We found that pure ZnO does not react with thiophene. Hence, Ni acts as a desulfurization catalyst producing from thiophene free sulfur species, which react further with ZnO. More detailed information on the role of Ni can be obtained from the comparison of the sample used in the present work with that studied previously, which contained 6 wt% of Ni and had a similar particle size (Table 3). The first stage is more rapid for the sample containing 12 wt% of Ni both in reduced and unreduced form. The rate of the second stage increases with Ni content, but only in the unreduced sample. For the reduced sample, unexpectedly, the rate of the second stage is slightly lower for the sample with higher Ni amount (ratio 0.9, see Table 3). It means that during the first stage, both in the reduced and unreduced samples, Ni is directly involved in the reaction, whereas the role of Ni in the second stage depends on the pretreatment. In the reduced sample the reaction is limited by a process that is not localized on Ni surface, while in the unreduced sample the reaction is controlled (at least partially) by a step located on Ni.

Our conclusion about desulfurization as the rate determining process for both stages of the reactive adsorption seems to be incompatible with dramatic changes (decrease of the reaction rate and activation energy, and change of the role of Ni) observed when passing from the first stage to the second one. It is worth reminding however that thiophene decomposition is a multi step process, which can be limited either by desulfurization reaction itself or by thiophene diffusion to the surface of the active phase. We suppose that the reactive adsorption occurs in two stages, because the relative rate of these two steps of thiophene decomposition varies in the course of reaction.

Higher activation energy and Ni involvement in the first stage allows to conclude that its rate limiting step is thiophene desulfurization reaction, which can proceed by HDS or by direct decomposition of chemisorbed thiophene on metallic Ni as it was previously observed [8,9]. Thus formed free sulfur species can replace oxygen transforming progressively ZnO into ZnS. As this transformation is accompanied by a strong increase of molar volume (from 14.3 to 23.8 cm^3/mol) and a pronounced agglomeration of particles, it leads to a collapse of the interparticle voids [10]. This textural evolution can slow down thiophene diffusion making it the rate determining step instead of desulfurization itself. Such a change of the rate determining step allows to account for the appearance of the second stage characterized by decrease of the reaction rate, drop of the activation energy and an insensitivity

Table 3
Ratios of the reaction rates for NiO/ZnO samples containing 12 and 6 wt% of Ni for the first (v_I) and second (v_{II}) stages

Temperature (°C)	Thiophene pressure (mbar)	Reduced		Unreduced	
		$v_I(12)/v_I(6)$	$v_{II}(12)/v_{II}(6)$	$v_I(12)/v_I(6)$	$v_{II}(12)/v_{II}(6)$
360	20	1.4	0.9	1.5	1.2
330	20	1.2	0.9	1.9	1.4
330	10	1.3	0.9	1.9	1.3
330	40	1.2	1	1.7	2.2

to Ni amount as observed for the reduced sample. The situation is more complex for the unreduced sample. After the first stage the reaction rate and activation energy in this sample also decrease (although to a lower extent than in the reduced one), but the reaction rate continues to depend on Ni amount. Such a behavior can be explained by a weaker diffusion resistance in such sample, so that thiophene transport slows down to a lesser extent than in the reduced sample. In such a case both steps, desulfurization itself and thiophene diffusion, can have similar rates and both control the rate of the second stage of the reaction.

The proposed outline of the reactive adsorption allows to explain the role of hydrogen pretreatment. The important characteristic of the reduced adsorbent is existence of the induction period. It means that Ni–Zn alloy, formed in this sample after pretreatment, has a low activity in thiophene desulfurization. It is only after sulfidation of Zn counterpart of the alloy that Ni is liberated and the desulfurization can proceed attaining a similar maximum rate as in the unreduced sample, which contains free Ni species from the beginning. After a partial sulfidation the reaction slows down and the effect is more pronounced for the reduced sample (Table 2). According to the proposed reaction scheme such a difference means that thiophene diffusion is hindered to a greater extent in the reduced sample. This effect can be due to formation of Ni particles through decomposition of Ni–Zn alloy and consequently their lower accessibility. Also, additional agglomeration of ZnO particles, induced by the reduction and reflected by a decrease of BET surface area (Table 1), can further decrease the accessibility of Ni particles.

Some conclusions relevant to industrial application of NiO/ZnO-type adsorbents can be drawn from our study. First interesting point is that NiO/ZnO adsorbents do not need to be reduced before use. Formation of metallic Ni from NiO, even in the presence of thiophene, is sufficiently rapid to provide an active phase for thiophene desulfurization. Moreover, if the adsorbent has to be used until complete sulfidation, the unreduced solid would show better performances due to a more rapid overall reaction. Another important point is a rate limiting nature of the thiophene desulfurization reaction. The fact that the first stage involves directly Ni means that in adsorbents that are used only during this rapid stage, improved performance can be achieved by increasing HDS activity. In contrast, if a complete sulfidation is envisaged, the texture of the sulfided solid should also be optimized in order to ameliorate the accessibility of the active phase.

5. Conclusions

We have shown that NiO/ZnO adsorbents can be used in the reactive adsorption of thiophene without any reductive pretreatment. Metallic Ni particles, active in catalytic thiophene decomposition, are formed rapidly upon the contact with the thiophene/H_2 reaction mixture. Moreover, the unreduced adsorbent reacts with thiophene two times more rapidly than the reduced one. The negative effect of reduction in hydrogen is attributed to a lower accessibility of Ni particles in the reduced solid.

Another part of this work concerns the characterization of the composition of the gas phase during NiO/ZnO sulfidation in a fixed bed reactor. We found that for both reduced and unreduced adsorbents hydrogen sulfide is absent in the gas phase until the reaction is completed. It means that under these conditions ZnO sulfidation is more rapid than thiophene decomposition, which is therefore the rate determining process of the reactive adsorption. Existence of two distinct reaction stages points out however that the elementary step, controlling thiophene decomposition, changes during reaction. We suggest that at the beginning the limiting step is the thiophene desulfurization itself, whereas after a partial sulfidation the thiophene diffusion becomes either a unique rate determining step (for the reduced sample) or controls the rate along with the desulfurization (for the unreduced sample).

Acknowledgement

A financial support from the Regional Council of Burgundy (FABER program) is gratefully acknowledged.

References

[1] M. Capone, fourth ed., Kirk Othmer Encyclopedia of Chemical Technology, vol. 23, John Wiley & Sons, Inc., New York, 1997, pp. 209–219.
[2] P.J.H. Carnell, in: M.V. Twigg (Ed.), Catalyst Handbook, second ed., Wolfe Publishing Ltd., London, 1989, pp. 191–224.
[3] H. Topsoe, B.S. Clausen, F.E. Massoth, in: J.R. Anderson, M. Boudart (Eds.), Hydrotreating Catalysis—Science and Technology, vol. 11, Springer-Verlag, Berlin, 1996.
[4] E. Ito, J.A. Rob van Veen, Catal. Today 116 (2006) 446–460.
[5] K. Tawara, T. Nishimura, H. Iwanami, T. Nishimoto, T. Hasuike, Ind. Eng. Chem. Res. 40 (2001) 2367–2370.
[6] I. Bezverkhyy, A. Ryzhikov, G. Gadacz, J.P. Bellat, Catal. Today 130 (2008) 199–205.
[7] N. Homs, J. Llorca, P.R. de la Piscina, Catal. Today 116 (2006) 361–366.
[8] G.R. Schoofs, R.E. Preston, J.B. Benziger, Langmuir 1 (1985) 313–320.
[9] F. Zaera, E.B. Kollin, J.L. Gland, Langmuir 3 (1987) 555–557.
[10] E.A. Efthimiadis, S.V. Sotirchos, Chem. Eng. Sci. 48 (1993) 429–843.